Acta Scientiarum
http://periodicos.uem.br/ojs
ISSN on-line: 1807-8664
Doi: 10.4025/actascitechnol.v46i1.63001

Bone regeneration in critical size calvarial defects using synthetic hydroxyapatite and mineralized bovine tendon base materials: a micro-computed tomography analysis

Maurício Bordini do Amaral[1], Rommel Bezerra Viana[2*], Katúcia Bezerra Viana[3], Cristina Aparecida Diagone[4], Aline Bassi Denis[4] and Ana Maria de Guzzi Plepis[4]

[1]Departamento de Bioengenharia, Universidade de São Paulo, São Carlos, São Paulo, Brazil. [2]Universidade Estadual do Ceará, Av. Dom Aureliano Matos, 2058, 62930-000, Limoeiro do Norte, Ceará, Brazil. [3]Centro de Ciências Biológicas e da Saúde, Universidade Federal do Estado do Rio de Janeiro, Rio de Janeiro, Rio de Janeiro, Brazil. [4]Instituto de Química de São Carlos, Universidade de São Paulo, São Carlos, São Paulo, Brazil. *Author for correspondence. E-mail: rommelbv@yahoo.com.br; rommel.viana@uece.br

ABSTRACT. This investigation used materials based on synthetic hydroxyapatite and mineralized bovine tendon as a framework for bone regeneration and evaluated the osteoconductivity of these materials in the calvaria of Wistar rats in comparison to Bio-Oss/Geistlich. Micro-computed tomography (μ-CT) analyses were performed non-invasively using three-dimensional image reconstruction to evaluate new bone formation; in addition, conventional histological analysis was used. The μ-CT results showed that Bio-Oss resulted in higher volume, density and bone percentage than the other materials. Based on the three-dimensional reconstructed images, the lowest resorption rates were observed in the Bio-Oss group, and the materials remained in larger quantities inside the defect at thirty days. In the synthetic hydroxyapatite group, intense resorption of the material and slight bone formation on the defect margins were noted, yielding an irregular edge. The mineralized bovine tendon group showed discrete new bone formation, and the material was fully resorbed. The Bio-Oss and synthetic hydroxyapatite groups yielded similar amounts of blood vessels and osteoblastic cells, and these were higher than the amounts found in the mineralized bovine tendon group. Synthetic hydroxyapatite was present within the defect and exhibited osteoconductive properties that were similar to the commercial brand, Bio-Oss. Mineralized bovine tendon did not exhibit good osteoconductivity and is contraindicated for maintaining bone space. Moreover, μ-CT yielded lower specificity; that is, μ-CT was not able to distinguish bone tissue from Bio-Oss, although it exhibited high sensitivity. Based on these results, it appears that synthetic hydroxyapatite has great potential for use in filling bone defects, unlike mineralized bovine tendon.

Keywords: biomaterials; bone graft; critical size defect; histological analysis.

Received on March 23, 2022.
Accepted on May 10 2023.

Introduction

Among synthetic materials, ceramics are the main product used for bone regeneration. Ceramics are considered biocompatible biomaterials that exhibit low traction but excellent compressive strength, high load resistance and low friction (Bahremandi-Toloue, Mohammadalizadeh, Mukherjee, & Karbasi, 2022; Ribas et al., 2019). The low-friction resistance is increased because ceramics are hydrophilic and can be well polished, increasing the ability of a surface to receive loads from other materials or from the body itself (Ribas et al., 2019). Although inorganic ceramics do not exhibit osteoinductive ability, they certainly exhibit an excellent osteoconductive ability and a remarkable ability to bind to bone. In this respect, bioactive ceramics comprise the largest family of alloplasts, namely: TriCalcium Phosphate (TCP), hydroxyapatite, calcium sulfate, and calcium carbonate; calcium hydroxide-based polymers; and bioactive glass ceramics (Ribas et al., 2019). Among these structures, hydroxyapatite and calcium phosphate are the main bioceramics used for hard tissue repair due to their similarity to natural bone minerals, excellent biocompatibility and bioactivity (Du, Chen, Liu, Xing, & Song, 2021; Zhi et al., 2022). In recent years, researchers have significantly improved the properties and performance of hydroxyapatite and calcium phosphate (Du et al., 2021; Zhi et al., 2022).

Scanning electron microscopy (SEM) is widely used to characterize bone substitutes and is very effective in the analysis of surface topography of materials, particularly their microscopic aspect, grain size and porosity. However, SEM does not provide data regarding the interior of samples. Often, estimates of microstructure obtained using SEM produce inaccurate results that are based only on the estimation of the surface; therefore, image analysis of the total porosity and volumetric load distribution by micro-computed tomography (µ-CT) is more effective (du Plessis & Broeckhoven, 2019; Irie et al., 2018). Currently, µ-CT analysis has been used to quantify bone morphology and the microstructure of biomaterials (Vásárhelyi, Kónya, Kukovecz, & Vajtai, 2020); consequently, many investigations have used µ-CT to evaluate the formation of mineralized matrix on several types of *in vitro* and *in vivo* biomaterials (Olăreț, Stancu, Iovu, & Serafim, 2021). It is worth noting that the µ-CT analysis can be used to quantify the architecture of polymeric frameworks by providing parameters such as porosity, interconnectivity and anisotropy; in addition, this technique can be used to evaluate other parameters involved in the mineralization process during bone repair (du Plessis & Broeckhoven, 2019; Irie et al., 2018). In addition, some studies have evaluated bone regeneration using µ-CT in critical size defects (Al-Hezaimi et al., 2016; Badwelan et al., 2021; Lappalainen et al., 2016), alveolar cleft (Kamal et al., 2017), osteochondral defects (Flaherty, Tamaddon, & Liu, 2021) and vascularized tissues (Redenski et al., 2022).

This study aims to evaluate the osteoconductive potential of experimental materials based on synthetic hydroxyapatite and mineralized bovine tendon. Considering that these materials are available in large quantities and in many shapes, they exhibit great potential for use in bone reconstruction. Thus, this study compares experimental hydroxyapatite and mineralized bovine tendon to an internationally known branded product (the commercially available Bio-Oss®) on a critical size bone defect. Another relevant aspect of this study is that it represents the development of a non-invasive method that showed the ability to quantify mineralized tissue at the site bone repair with high resolution, obtaining many clarifying images in a simple and effective way. In this context, the use of µ-CT represents a useful alternative for the evaluation of implants and vital structures.

Material and methods

The bone graft biomaterial Bio-Oss is produced by Geistlich Pharma (Switzerland). According to the manufacturer, Bio-Oss is obtained from inorganic bovine trabecular bone and is deproteinized at approximately 300ºC. Hydroxyapatite was synthesized using a 1.00 mol L^{-1} solution of $Ca(NO_3)_2.4H_2O$ and a 0.60 mol L^{-1} solution of $(NH_4)_2HPO_4$; the pH of the solutions was adjusted to lie between 11.0 and 12.0 using concentrated NH_4OH. The synthesis was carried out under a nitrogen atmosphere, and the size of the resulting particles was less than 0.2 mm.

Mineralized bovine tendon was obtained by treating tendon in an alkaline solution containing K^+, Na^+ and Ca^{2+} salts for 96 h at 25ºC (4 mL g^{-1} of material). The tendon was then balanced in a saline solution and then rinsed in H_3BO_3, EDTA and water (6 mL g^{-1} of material). The resulting matrices were mineralized in a solution containing 0.2 mol L^{-1} $CaCl_2$, pH 7.4 and 0.12 mol L^{-1} Na_2HPO_4, pH 9 for 6 h; the solution was replaced every 30 min., and the tendon was rinsed with deionized water between replacements. After mineralization, the matrices were frozen and lyophilized. All experimental materials were sterilized using ethylene oxide.

The bovine tendon was subjected to thermogravimetric analysis (TGA) under an air atmosphere at 10ºC $min^{-.1}$ in a TGA-2050 (TA Instruments, USA) device to determine the mineralization percentage. Differential scanning calorimetry measurements (DSC) were conducted under a dynamic air atmosphere (60 mL $min.^{-1}$) using a DSC 2010 (TA Instruments) device. SEM analyses were conducted using a 20 kV electron beam, and photomicrographs of the matrices were obtained under 100 and 500X magnification using a LEO 440 (LEO Electron Microscope) device equipped with an Oxford detector (Oxford Instruments). X-ray diffraction patterns were obtained using a Universal Carl Zeiss-Jena diffractometer and an X-ray source: Mod. URD-6, with 40 kV power, 20 mA and radiation of 1.5406 Å.

Biological analyses

Male adult Wistar rats, each weighing approximately 200 g, were divided into five groups, each comprising five animals, on which the surgical procedures were performed; the lesions were filled with different materials in each group. Radiographic and morphological analyses were conducted after 30 days. The lesions were filled with the following materials: Bio-Oss, synthetic hydroxyapatite, mineralized bovine tendon, the control group (lesion filling with clot) and the intact group (the animals were not subjected to surgery).

The surgeries were performed under general anesthesia using an intramuscular ketamine hydrochloride injection (Ketalar injection, Achë Laboratórios Farmacêuticos S.A., Brazil) at a dose of 75 mg kg^{-1} of body mass and the muscle relaxant and animal sedative Ropun (Bayer S.A., Brazil) at a dose of 1.5 mL kg^{-1} (see Figures 1 and 2).

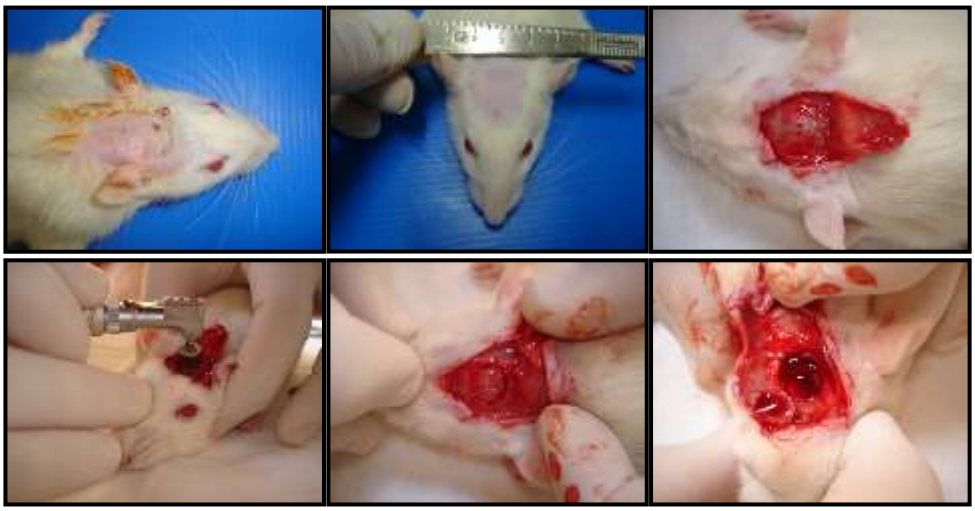

Figure 1. Description of surgical procedure: sterilization of the surgical field with povidone-iodine, trichotomy of the frontoparietal region, incision of tegument, complete detachment of the periosteum exposing the bone of the skull and trepanation using a trephine drill of 8 mm diameter. A view of the bicortical bone defect and exposure of the dura mater.

Figure 2. Filling the bone cavity with the tested materials: synthetic hydroxyapatite (A), mineralized bovine tendon (B) and Bio-Oss (C).

After trichotomy of the frontoparietal region of the head, vigorous sterilization was performed using povidone-iodine and local infiltration anesthesia with 2% lidocaine with norepinephrine 1:50,000 (Merrell Lepetit Farmacêutica e Industrial Ltda, Brazil). Semilunar incisions were carried out of the total thickness using a #15 blade on the integument of the skull lining, followed by flap detachment and exposure of the bone surface. Then, using a surgical trephine drill (8 mm diameter), an 8-mm diameter hole was made in the frontoparietal region (under abundant and continuous irrigation with saline solution), crossing through the entire diploe bone thickness and exposing the meninges in the back of the lesion. The lesion was filled with one of the materials used in this study, and the flap was then placed in position and sutured using #3 thread (Ethicon – Johnson & Johnson). Throughout the experimental period (30 days), the animals were housed in the vivarium and received food and water *ad libitum*. This period is appropriated for bone regeneration of critical defects as can be seen elsewhere (Brassolatti et al., 2021; Efeoglu et al., 2009; Pripatnanont, Nuntanaranont, Vongvatcharanon, & Limlertmongkol, 2007).

The animal model used for evaluating bone regeneration must meet certain criteria, including the following: the defect size cannot be smaller than the critical size for each species as reported in the literature; the methodology should not be too costly; the surgical technique should not be too complex; the implantation site should contain cortical and cancellous bone; the method should involve low morbidity, graft stability and impossibility of fracture; and finally, the method should quantify the regenerated tissue and the remainder of the implant from both radiographic and histological perspectives (Gauthier et al., 2005; Gielkens et al., 2008; Kochi et al., 2009).

This research was approved by the Ethics Committee on Animal Experiments of the Ribeirão Preto Medical School at the University of São Paulo at a meeting on March 30, 2009 (process number 028/2009; attached).

Finally, the animals were killed using an overdose of ketamine hydrochloride (Ketalar injection – Achë Laboratórios Farmacêuticos S.A., Brazil) 30 days after surgery. The cranial caps were immediately dissected, placed in individual vials, labeled, and fixed in 10% formalin in phosphate buffer, pH 7.2, for 7 days.

Histological and µ-CT analyses

Radiographic analyses were conducted using micro-computed tomography, which was implemented using a SkyScan (100 kV – 100 µA) micro-tomography scanner. The animals were positioned and fixed to the machine saddle such that they could not move during the experiment because any movement would prevent image acquisition. The device was set to a resolution of 2,000 x 2,000 pixels and 16 µm-thick sections. The acquisition time of the images was approximately 2h per sample. The images were analyzed and reconstructed in two and three dimensions, and newly formed bone tissue was quantified using the *Software CTAnalyser Version*. After the radiographic images were acquired, a circular region of interest (8 mm in diameter) was selected for analysis (at a thickness that comprised the calvarial bone diploë). The diameter of the region of interest was 8 mm to ensure that bone regeneration inside the critical size defect was fully analyzed.

For the three-dimensional image analysis, the gray scale (*gray threshold*) was first fine-tuned. The gray value of an image is proportional to the linear attenuation coefficient of the tissue. The gray-scale values used in the analysis program ranged from 0 to 255. In this study, the lowest gray-scale value used was 90, and the highest was 250. Thus, it was possible to differentiate mineralized hard tissue from soft tissue, especially inside the 8-mm critical defect.

The morphometric quantitative analysis of the tissue inside the bone defect was conducted in pixels corresponding to mineralized tissue, excluding non-mineralized soft tissue. Three-dimensional images were reconstructed for each sample, and the following morphometric parameters were obtained: (a) the volume of bone tissue, which refers to the amount of mineralized tissue present within the defect (BV; mm^3); (b) the percentage of bone tissue, which refers to the ratio of the mineralized tissue volume to the total analyzed volume (BV/TV; %); (c) the bone contact surface associated with the interconnected mineralized tissue surface area (mm^2); (d) and bone surface density, which is related to the ratio of the total mineralized tissue surface area to the total analyzed volume (BS/TV).

Subsequently, the samples were decalcified in MORSE solution (50% formic acid + 10% sodium citrate, 1:1) for 30 days. After histological processing, the pieces were embedded in Histosec (paraffin + synthetic resin); the samples were oriented such that histological sections were obtained in the lateral-lateral direction. Semi-serial sections of 5 µm in thickness were obtained and stained using the hematoxylin-eosin technique. The slide sections were evaluated and photographed using a Leica Leitz DM RX microscope equipped with an image analysis system. The following aspects of tissue reaction were observed in the histomorphometric analysis: (i) newly formed bone tissue, which refers to the young bone tissue formed in the defect area, especially at the margins; (ii) the remaining biomaterial, which refers to biomaterial particles remaining inside the defect, indicating the rate of resorption; (iii) neovascularization, which describes the blood capillaries around the biomaterial and inside the defect; (iv) connective tissue, which describes the presence of connective tissue within the defect; (v) osteoblastic cells, which describes the presence of bone-forming cells, including osteoblasts, osteocytes and remodeling cells, such as osteoclasts.

During the histological analysis, the analyzed tissue parameters were accorded a semi-quantitative score based on the following criteria: (0) none; (1) minimum; (2) moderate; (3) well-established and (4) intense.

Statistical analysis

While comparing the materials using µ-CT, it was found that the groups presented a normal distribution according to the Kolmogorov-Smirnov test. Then, an analysis of variance was performed using a fixed model criterion (for each measurement); when significant differences were found, the *post-hoc* Tukey's test was used for multiple comparisons. To compare the materials based on the histological evaluation, it was first verified that the groups were not normally distributed according to the Kolmogorov-Smirnov test. For each measurement, when the Kruskal-Wallis test indicated a significant difference, the *post-hoc* Dunn's test was used for multiple comparisons. To verify correlations between the µ-CT measurements and the conventional histological evaluations, Spearman's correlation coefficient was used. In all statistical tests, a significance level of 5% was adopted ($p < 0.05$).

Results and discussions

Several studies suggest that tomographic section thicknesses should be between 9.4 to 18 µm (Cacciafesta, Dalstra, Bosch, Melsen, & Andreassen, 2001; Verna, Bosch, Dalstra, Wikesjö, & Trombelli, 2002), whereas other studies suggest a section thickness of 25 µm (Jones et al., 2004). Thus, in this study, an intermediate tomographic section thickness was used (16 µm). Another notable consideration is the diameter of the rat calvaria defect. In this study, a defect of 8 mm in diameter was created, corresponding to a critical size defect that does not heal completely throughout the animal's life (Jensen, Schou, Stavropoulos, Terheyden, & Holmstrup, 2012). In this study, greater growth was observed from the margins on the dura mater (with a ramp aspect) for all groups. However, the healing of the calvarial defect normally begins at the margins of the surgical wound (from the underlying dura mater or overlying periosteum), and the higher the osteoconductive capacity of the material, the greater the growth that is observed (Pripatnanont et al., 2007).

Based in thermogravimetric curves for the mineralized and non-mineralized bovine tendons (Figure 3a), the mineralized matrix yielded 60.9% residue at a temperature of 750°C, which is derived from inorganic material deposited on the tendon. This loss of approximately 40% of the mass corresponds to the organic constituent, which is derived from bovine collagen. In contrast, Bio-Oss comprises a small amount of organic constituents, consisting mainly of bovine hydroxyapatite (Jensen et al., 2012).

The differential scanning calorimetry curves for the bovine tendons (mineralized and mineralized/sterilized) shows no significant energy variations were observed for the inorganic materials at this temperature, except in the mineralized bovine tendon (Figure 3b). The denaturation temperatures were as follows: bovine tendon (46.7°C), mineralized bovine tendon (59.0°C) and mineralized and sterilized bovine tendon (56.1°C). Temperatures of approximately 40°C correspond to collagen denaturation (Ogawa & Plepis, 2002).

Figure 4(a,b) shows SEM micrographs of the mineralized bovine tendon surface. The structural images of the surface and cross section of the mineralized bovine tendon show that several mineral granules are deposited on the organic matrix, and the observed irregular shape with pores indicates a favorable environment for cell repopulation. SEM images of Bio-Oss (Figure 4 (c,d)) show a highly porous material that allows cell and vascular growth in its interior; by examining the trabecular, the framework for conduction and space maintenance for bone growth can be observed.

In respect of the biological evaluation, all animals showed excellent recovery in the days after the surgery, and no anti-inflammatory agents or antibiotics were required. In the control group (not subjected to surgery), the animals were evaluated using µ-CT. Figure 5 shows three-dimensional images obtained using µ-CT of the cranial anatomy of the control group (surgery without graft). In the control group, the bone defect created by surgery persisted, and no new bone tissue was formed. This result shows that this type of defect does not spontaneously regenerate without the use of regenerative therapies. The 8-mm circular defect remained almost unchanged, with only the faintest irregularity observed in the outline (Figure 5b).

In the bovine tendon and synthetic hydroxyapatite experimental groups (one month after surgery), intense resorption of biomaterials and the discrete formation of mineralized tissue was observed in all cases according to µ-CT images (see Figure 6); the defect space was probably filled with connective tissue. It is possible to see centripetal closure of the surgical wound with very irregular edges (showing new bone formation) and the presence of white spots floating inside the defect, representing almost fully resorbed hydroxyapatite. The lateral edges of the bone defect have a beveled aspect, indicating the start of new bone formation. However, none of the animals exhibited an exacerbated inflammatory response with intense bone resorption, which would contraindicate the use of these materials. Importantly, due to the chemical similarity of bovine hydroxyapatite and hydroxyapatite in the calvarial bone of the animal, it was not possible to differentiate the adjacent remainder of the bone tissue. The synthetic hydroxyapatite granules that were at the resorption stage inside the defect were not observed in the µ-CT analysis and therefore were not considered mineralized tissue. The calcium phosphate from the mineralized bovine tendon was completely reabsorbed at the end of the period according to µ-CT, thus corroborating the histological analysis findings. However, closure of the surgical wound with irregular margins was observed, indicating the resorption process (concavity) and new bone formation (extensions); the mineralized tendon was almost completely reabsorbed.

The graft was slowly reabsorbed, thereby providing a framework for tissue growth therein and the formation of new bone tissue; however, many Bio-Oss granules remain inside the defect that have not yet been reabsorbed (see Figure 7). In the last animal, an unfavorable tissue reaction was observed, and the graft was eliminated; in this case, there was moderate bone resorption extending from the edge of the wound and little new bone formation.

Mineralized tissue was strongly present, almost completely closing the bone defect. This material comprising inorganic bovine bone was not quickly reabsorbed, allowing the bone tissue space to remain. Moreover, no invagination of the connective tissue was observed, thus allowing new bone formation.

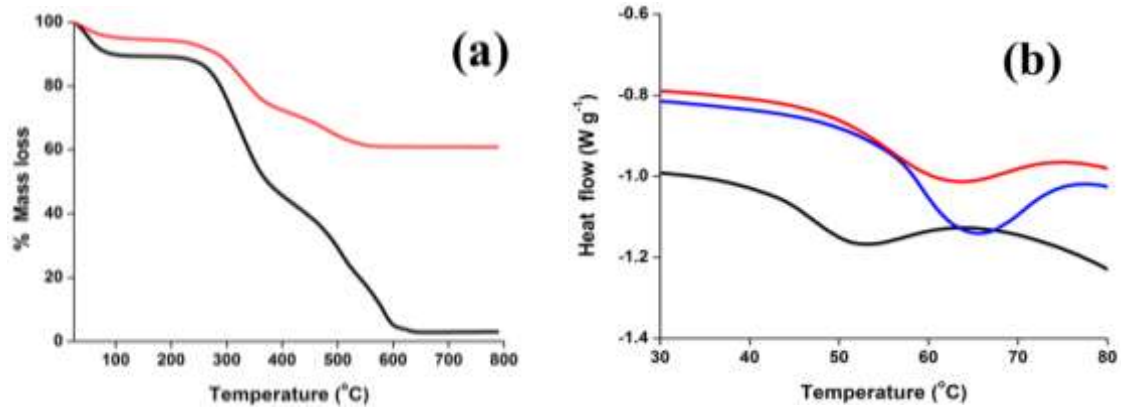

Figure 3. (a) Thermogravimetric curves for mineralized and non-mineralized bovine tendon (air, 10°C min^{-1}). Black indicates the analysis of bovine tendon subjected to alkaline treatment for 96 h. Red indicates the analysis of mineralized bovine tendon subjected to alkaline treatment for 96 h. (b) Differential Scanning Calorimetry curves for bovine tendon (black), mineralized bovine tendon (blue) and mineralized and sterilized bovine tendon (red).

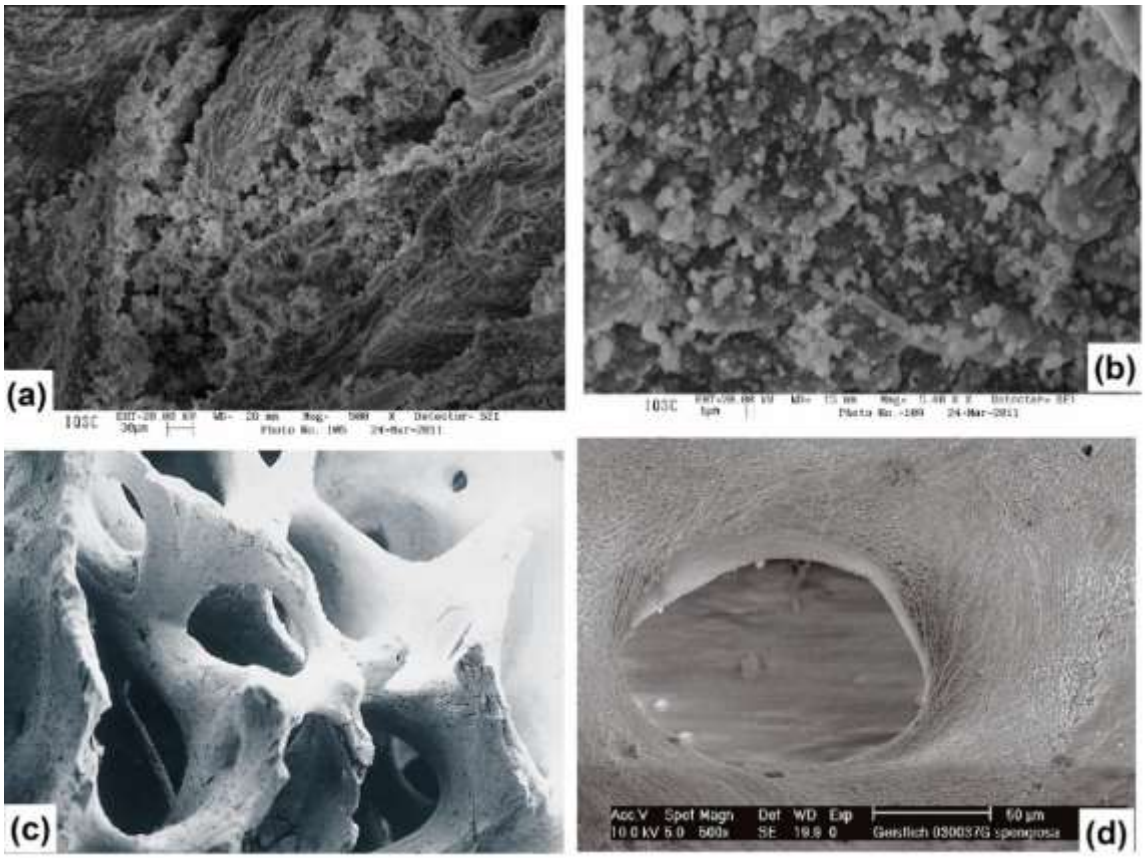

Figure 4. SEM of surfaces: (a) Mineralized bovine tendon (500x magnification). (b) Mineralized bovine tendon (5,000x magnification). (c) Cross section of Bio-Oss (50x magnification). (d) Cross section of Geistlich Bio-Oss (500x magnification).

Table 1 shows a comparison of the three studied materials based on µ-CT measurements. Based on a statistical analysis of the µ-CT results for the three materials, Bio-Oss resulted in the highest volume of bone tissue; that is, the Bio-Oss particles remained inside the defect and were less resorbed. Thus, this biomaterial exhibited better osteoconductivity; by remaining inside the defect, this material avoided connective tissue invagination and provided a framework for bone growth. The same result was observed when analyzing bone tissue percentage (the ratio of bone tissue volume to the total analyzed volume), emphasizing yet again that the Bio-Oss group resulted in a greater amount of mineralized tissue.

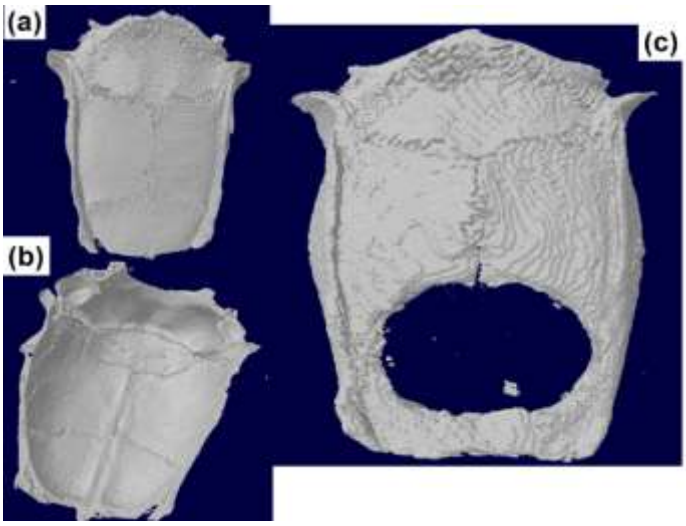

Figure 5. Three-dimensional images obtained using µ-CT: (a,b) Cranial anatomy of a Wistar rat (intact control). (c) Three-dimensional image of the control surgery without grafting after 30 days.

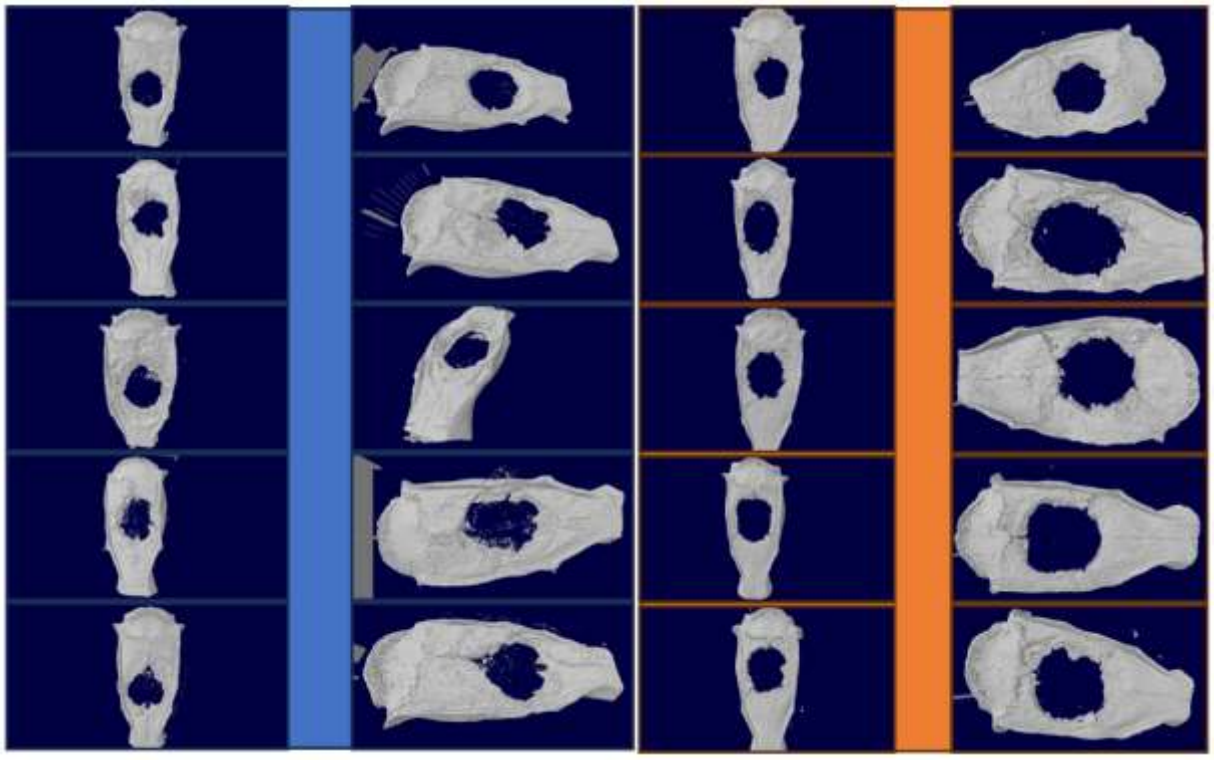

Figure 6. Three-dimensional images obtained using µ-CT of the bone repair of sites grafted with synthetic hydroxyapatite (blue background) and mineralized bovine tendon (orange background) after 30 days of healing.

Bone surface contact (representing the surface area of the interconnected mineralized tissue) was also evaluated using µ-CT. Bone tissue interconnectivity is an important requirement because the contact between the granules provides a conduit for the entry of osteoblastic cells, blood vessels and hard tissue growth (Cacciafesta et al., 2001; Jones et al., 2004; Verna et al., 2002). Bio-Oss exhibited a greater contact surface than hydroxyapatite, followed in turn by bovine tendon. µ-CT analysis also provided the bone surface density, which is the ratio of total mineralized tissue surface area to the total analyzed volume. Bio-Oss exhibited greater bone surface density than the other materials; that is, the Bio-Oss group had a larger mineralized surface area than the other groups. Synthetic hydroxyapatite has a porous microstructure that contains a n etwork of interconnected points with sizes ranging between 200 and 500 µm, thus providing a framework for the entry of osteogenic cells and blood capillaries. These characteristics are similar to those of inorganic bovine bone that is synthesized at low temperature, such as Bio-Oss. Thus, for the osteoblasts to proliferate the inside the material, a single cell requires contact with at least three other cells through an interconnected network of pores, which must be at least 100 µm in diameter

[approximately three times the size of the osteoblast (30 µm)] (Wang et al., 2004). According to Wang et al. (2004), a structure with pores ranging from 200 to 400 µm allows cell growth and differentiation in its interior and facilitates their nutrition through blood capillaries.

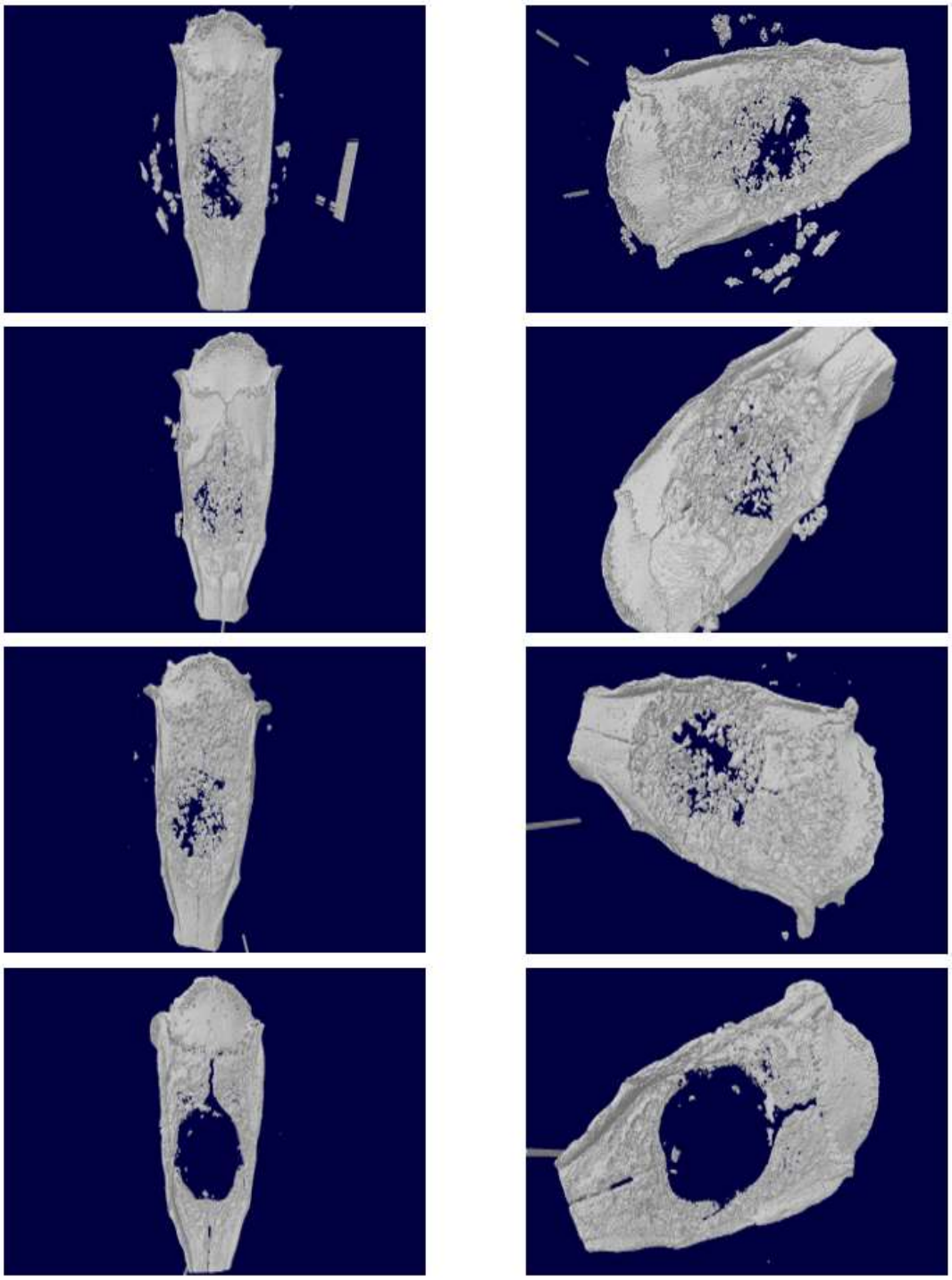

Figure 7. Three-dimensional images obtained using µ-CT of the bone repair of sites grafted with Bio-Oss after 30 days of healing.

Table 1. Comparison of the three tested materials according to measurements obtained using µ-CT.

Parameter	Bio-Oss		Hydroxyapatite		Tendon		p
	Mean	sd	Mean	sd	Mean	sd	
Bone tissue volume	20.59 [a]	4.56	5.35 [b]	2.52	1.86 [b]	1.44	<0.001 *
Bone tissue percentage	11.49 [a]	2.88	3.05 [b]	1.42	1.09 [b]	0.89	<0.001 *
Contact surface	15.98 [a]	2.48	9.34 [b]	2.7	4.01 [c]	3.8	<0.001 *
Bone surface density	2.08 [a]	0.46	0.80 [b]	0.34	0.31 [b]	0.18	<0.001 *

* Significant difference ($p < 0.05$). Materials with the same letters are not significantly different from each other.

After 30 days, the defects filled with Bio-Oss exhibited a large amount of particulate matter inside the defect, which was surrounded by connective tissue containing many cells and a large number of blood vessels. Many osteoblastic cells can be observed around the material in the photomicrograph of the Bio-Oss defect; however, in newly formed bone tissue, these osteoblasts were found mainly on the margins of the defect and near the dura mater. Low degradation of Bio-Oss particles has been reported fifteen months after grafting of the maxillary sinus in humans (Busenlechner et al., 2009). More pronounced Bio-Oss degradation (with only a few particles remaining after six months) has been reported in only one study (Terheyden, Jepsen, Möller, Tucker, & Rueger, 1999). In other study (Kuchler et al., 2013), there was no statistically significant difference in the proportion of the remaining particles of Bio-Oss between 7 and 18 months. This evidence of slow degradation justifies the large number of Bio-Oss particles found inside the defect in our study.

During the same period, synthetic hydroxyapatite exhibited a large amount of remaining material, although the particle size was smaller than for the Bio-Oss particles. We also observed cell-rich connective tissue containing a large number of blood vessels; however, the presence of newly formed bone tissue and the number of osteoblastic cells were less obvious. These results corroborate the findings of Pallesen et al. (2002), who showed that hydroxyapatite particles with diameters of 0.5 to 2 mm are more suitable for bone regeneration than 10 mm particles. Hydroxyapatite particle size also appears to affect the osteogenic potential of mesenchymal stem cells, as observed in the *in vitro* study by Weissenboeck et al. (2006); in that study, the authors found that small particles exhibited high levels of specific alkaline phosphatase activity.

It is noteworthy to mention that the mineralized bovine tendon was almost entirely resorbed, making way for abundant connective tissue containing few cells. In this case, the blood vessels were not present in large amounts, and almost no osteoblastic cells and newly formed bone tissue were found. O'Hara et al. (2012) investigated the incorporation of calcium phosphate into collagen fibers that were derived from bovine tendon *in vitro*. In that study, O'Hara et al. (2012) suggested the potential of this composite for use in the treatment of vertebral fractures; however, *in vivo* studies would be required to provide clinical evidence of its effectiveness, especially regarding degradation. The results of this *in vivo* investigation showed that this composite is rapidly resorbed; therefore, some improvements are needed in its composition to improve its clinical performance (O'Hara et al., 2012).

In the control group (filled only with a blood clot), bone tissue space was lost, and few cells and vessels were present in the connective tissue; minimal amounts of newly formed tissue were present on the margins of the defect, showing the permanent nature of the defect. These results showed that in the control group (with blood clot only), there was no bone healing in the center or even at the periphery of the defect; this result confirms earlier studies showing that clot alone yields minimum bone formation at the periphery, even over long periods (Lee et al., 2010; Lu & Rabie, 2004). He, Yan, Chen, and Lu (2008) and Huh et al. (2005) also observed limited bone formation at the periphery of the defect in the control group. Schmitz, Schwartza, Hollinger, and Boyan (1990) described the behavior of cells in the critical size defect, noting that the release of growth factors (such as bone morphogenetic proteins) from the margin of the defect led to the differentiation of mesenchymal cells into osteoblasts. These cells form and mineralize the bone matrix by creating mineral islands that serve as a substrate for the growth of new bone tissue (Schmitz et al., 1990). However, due to the lack of growth and nutrition factors in the control group, not much osteoblast differentiation and bone formation was found beyond the wound margins. Thus, osteoblasts are not able to form and mineralize the bone matrix, leading to the formation of fibrous connective tissue (Ruehe, Niehues, Heberer, & Nelson, 2009).

Table 2 shows a comparison between the three materials based on conventional histological evaluation. The Bio-Oss material resulted in higher amounts of newly formed bone tissue than hydroxyapatite, which in turn was more effective than tendon. Although these numerical results were very clear, they were not statistically significant. This might be the case because bone tissue mineralizes slowly, and the process was not fully concluded during the study period. Nevertheless, Bio-Oss exhibited a higher osteoconductive capacity than hydroxyapatite and tendon, in that order. Osteoconductivity is an essential prerequisite for future bone formation.

Regarding the presence of biomaterials inside the defect, Bio-Oss and hydroxyapatite presented statistically similar results, and both cases exhibited a significant difference from the mineralized tendon (Table 2). Bio-Oss and hydroxyapatite remained within the defect during the evaluation period similarly, but the Bio-Oss granules were larger and were slightly more numerous than the hydroxyapatite granules. The mineralized tendon was almost fully resorbed during the evaluation period and showed a statistically

significant difference from the other groups. The mineralized tendon underwent significant resorption at 30 days and was not able to retain the space for bone growth, demonstrating its poor osteoconductivity. Although the mineralized tendon group exhibited a higher amount of connective tissue than the other groups, the results were not statistically significant. The connective tissue in the tendon group presented fewer cells and vessels; in the other groups, the connective tissue presented abundant tissue repair cells and blood vessels, indicating the regenerative nature of the lesion.

Table 2. Comparison of the three materials according to measurements obtained using conventional histological evaluation.

Parameter	Bio-Oss			Hydroxyapatite			Tendon			p
	Mean	med	sqr	Mean	med	sqr	Mean	med	sqr	
Newly formed bone tissue	2.3	2.5	0.8	1.6	2.0	0.5	1.2	1.0	0.0	0.142^{ns}
Presence of biomaterial	2.8 [a]	3.0	0.8	2.2 [a]	2.0	0.5	1.0 [b]	1.0	0.0	0.025*
Connective tissue	2.5	2.0	0.5	2.6	3.0	0.5	3.0	3.0	0.0	0.292^{ns}
Blood vessels	2.0 [a]	2.0	0.0	2.0 [a]	2.0	0.0	1.2 [b]	1.0	0.0	0.001*
Osteoblastic cells	2.3 [a]	2.5	0.8	1.6 [a]	2.0	0.5	1.0 [b]	1.0	0.0	0.042*

med = median. sqr = semi-quartile range. * Significant difference ($p < 0.05$). ns - Non-significant difference. Materials with the same letters are not significantly different from each other

The relationship between angiogenesis and osteogenesis plays an important role in bone formation. Several studies have shown that osteogenesis depends on angiogenesis, and tissue oxygen tension determines the differentiation of mesenchymal cells into osteoblasts or chondroblasts (Gerber & Ferrara, 2000; Hausman, Schaffler, & Majeska, 2001; Pelissier et al., 2003). Because these blood vessels are extremely important for bone formation, these vessels were also measured in the histological analysis. The Bio-Oss and the hydroxyapatite groups did not significantly differ, but the tendon group presented significantly fewer vessels. Thus, Bio-Oss and hydroxyapatite are advantageous for osteogenesis due to the presence of blood vessels (Table 2). In addition, due to their similarity to natural bone minerals, hydroxyapatite and Bio-Oss showed excellent biocompatibility, osteogenic capacity and bioactivity (Chu, Orton, Hollister, Feinberg, & Halloran, 2002; Pilliar, Filiaggi, Wells, Grynpas, & Kandel, 2001). In contrast, the mineralized tendon exhibited connective tissue that tended to stabilize due to the reduced number of blood vessels.

The Bio-Oss and hydroxyapatite groups presented higher numbers of osteoblastic cells, and no statistically significant difference was apparent between them. The mineralized tendon group exhibited significantly fewer osteoblastic cells. The inorganic bovine bone, hydroxyapatite and calcium phosphate derivatives have excellent osteoinductive properties that appear to stimulate the differentiation and proliferation of osteoblasts, particularly in critical size defects, because the calvaria contains a small amount of bone marrow (Chen, Shih, Lin, & Lin, 2004). Sohier, Daculsi, Sourice, De Groot, and Layrolle (2010) implanted bone morphogenetic protein, which was associated with calcium phosphate in the muscles of rats; the authors reported bone formation in the presence of calcium phosphate that was twelve times higher than that observed in the presence of morphogenetic bone protein alone. Therefore, due to the osteoinductive character and persistence of the material inside the defect, Bio-Oss and hydroxyapatite showed the highest number of osteoblasts. Although the mineralized tendon included calcium phosphate in its composition, this does not appear to have significantly affected the recruitment of osteoblasts, probably because the amount of mineral in the material was small.

Conclusion

In a radiographic assessment, the Bio-Oss exhibited better osteoconductivity than the other experimental materials. Histological examinations showed that synthetic hydroxyapatite was present inside the defect and exhibited osteoconductive properties that were similar to Bio-Oss. The mineralized bovine tendon did not exhibit good osteoconductivity and synthetic hydroxyapatite exhibited great potential for use in filling bone defects. When comparing the two methodologies, μ-CT presented low specificity but high sensitivity while histological analysis was able to accurately distinguish the tested materials from the adjacent tissue, but it was not possible to quantify the materials easily and accurately.

Acknowledgements

We would like to thank the Laboratory of Biochemistry and Biomaterials of the Institute of Chemistry of São Carlos (USP) and the bioengineering laboratory and animal facilities of the São Carlos School of

Engineering (USP). We would also like to thank Nelson Ferreira da Silva Júnior (USP) for his assistance with several surgeries and with the treatment of the animals, Dr. Alessandro Márcio Hakme da Silva for his assistance in the micro-computed tomography analysis, and Prof. Vanda Jorgete (Hospital das Clínicas, USP) for her assistance with the histological analyses. R.B. Viana acknowledges Alagoas Research Foundation/National Council of Scientific and Technological Development (FAPEAL/CNPq) for PDCTR research fellowship (313686/2022-0)

References

Al-Hezaimi, K., Ramalingam, S., Al-Askar, M., Arrejaie, A. S., Nooh, N., Jawad, F., ... Wang, C. Y. (2016). Real-time-guided bone regeneration around standardized critical size calvarial defects using bone marrow-derived mesenchymal stem cells and collagen membrane with and without using tricalcium phosphate: An in vivo micro-computed tomographic and histologic. *International Journal of Oral Science*, *8*, 7-15. DOI: https://doi.org/10.1038/ijos.2015.34

Badwelan, M., Alkindi, M., Alghamdi, O., Ahmed, A., Ramalingam, S., & Alrahlah, A. (2021). Bone Regeneration Using PEVAV/β-Tricalcium Phosphate Composite Scaffolds in Standardized Calvarial Defects: Micro-Computed Tomographic Experiment in Rats. *Materials 2021*, *14*(9), 2384. DOI: https://doi.org/10.3390/MA14092384

Bahremandi-Toloue, E., Mohammadalizadeh, Z., Mukherjee, S., & Karbasi, S. (2022). Incorporation of inorganic bioceramics into electrospun scaffolds for tissue engineering applications: A review. *Ceramics International*, *48*(7), 8803-8837. DOI: https://doi.org/10.1016/j.ceramint.2021.12.125

Brassolatti, P., Bossini, P. S., De Andrade, A. L. M., Flores Luna, G. L., Da Silva, J. V., Almeida-Lopes, L., ... De Freitas Anibal, F. (2021). Comparison of two different biomaterials in the bone regeneration (15, 30 and 60 days) of critical defects in rats. *Acta Cirurgica Brasileira*, *36*(6). DOI: https://doi.org/10.1590/ACB360605

Busenlechner, D., Huber, C. D., Vasak, C., Dobsak, A., Gruber, R., & Watzek, G. (2009). Sinus augmentation analysis revised: The gradient of graft consolidation. *Clinical Oral Implants Research*, *20*(10), 1078-1083. DOI: https://doi.org/10.1111/j.1600-0501.2009.01733.x

Cacciafesta, V., Dalstra, M., Bosch, C., Melsen, B., & Andreassen, T. T. (2001). Growth hormone treatment promotes guided bone regeneration in rat calvarial defects. *European Journal of Orthodontics*, *23*(6), 733-740. DOI: https://doi.org/10.1093/ejo/23.6.733

Chen, T. M., Shih, C., Lin, T. F., & Lin, F. H. (2004). Reconstruction of calvarial bone defects using an osteoconductive material and post-implantation hyperbaric oxygen treatment. *Materials Science and Engineering C*, *24*(6-8 SPEC. ISS.), 855-860. DOI: https://doi.org/10.1016/j.msec.2004.08.040

Chu, T. M. G., Orton, D. G., Hollister, S. J., Feinberg, S. E., & Halloran, J. W. (2002). Mechanical and in vivo performance of hydroxyapatite implants with controlled architectures. *Biomaterials*, *23*(5), 1283-1293. DOI: https://doi.org/10.1016/S0142-9612(01)00243-5

Du, M., Chen, J., Liu, K., Xing, H., & Song, C. (2021). Recent advances in biomedical engineering of nano-hydroxyapatite including dentistry, cancer treatment and bone repair. *Composites Part B: Engineering*, *215*, 108790. DOI: https://doi.org/10.1016/j.compositesb.2021.108790

du Plessis, A., & Broeckhoven, C. (2019). Looking deep into nature: A review of micro-computed tomography in biomimicry. *Acta Biomaterialia*, *85*, 27-40. DOI: https://doi.org/10.1016/j.actbio.2018.12.014

Efeoglu, C., Burke, J. L., Parsons, A. J., Aitchison, G. A., Scotchford, C., Rudd, C., ... Fisher, S. E. (2009). Analysis of calvarial bone defects in rats using microcomputed tomography: potential for a novel composite material and a new quantitative measurement. *British Journal of Oral and Maxillofacial Surgery*, *47*(8), 616-621. DOI: https://doi.org/10.1016/j.bjoms.2009.02.010

Flaherty, T., Tamaddon, M., & Liu, C. (2021). Micro-computed tomography analysis of subchondral bone regeneration using osteochondral scaffolds in an ovine condyle model. *Applied Sciences (Switzerland)*, *11*(3), 1-14. DOI: https://doi.org/10.3390/app11030891

Gauthier, O., Müller, R., Von Stechow, D., Lamy, B., Weiss, P., Bouler, J. M., ... Daculsi, G. (2005). In vivo bone regeneration with injectable calcium phosphate biomaterial: A three-dimensional micro-computed

tomographic, biomechanical and SEM study. *Biomaterials*, *26*(27), 5444-5453. DOI: https://doi.org/10.1016/j.biomaterials.2005.01.072

Gerber, H. P., & Ferrara, N. (2000). Angiogenesis and bone growth. *Trends in Cardiovascular Medicine*, *10*(5), 223-228. DOI: https://doi.org/10.1016/S1050-1738(00)00074-8

Gielkens, P. F. M., Schortinghuis, J., de Jong, J. R., Huysmans, M. C. D. N. J. M., Leeuwen, M. B. M. va., Raghoebar, G. M., ... Stegenga, B. (2008). A comparison of micro-CT, microradiography and histomorphometry in bone research. *Archives of Oral Biology*, *53*(6), 558-566. DOI: https://doi.org/10.1016/j.archoralbio.2007.11.011

Hausman, M. R., Schaffler, M. B., & Majeska, R. J. (2001). Prevention of fracture healing in rats by an inhibitor of angiogenesis. *Bone*, *29*(6), 560-564. DOI: https://doi.org/10.1016/S8756-3282(01)00608-1

He, H., Yan, W., Chen, G., & Lu, Z. (2008). Acceleration of de novo bone formation with a novel bioabsorbable film: A histomorphometric study in vivo. *Journal of Oral Pathology and Medicine*, *37*(6), 378-382. DOI: https://doi.org/10.1111/j.1600-0714.2008.00651.x

Huh, J. Y., Choi, B. H., Kim, B. Y., Lee, S. H., Zhu, S. J., & Jung, J. H. (2005). Critical size defect in the canine mandible. *Oral Surgery, Oral Medicine, Oral Pathology, Oral Radiology and Endodontology*, *100*(3), 296-301. DOI: https://doi.org/10.1016/j.tripleo.2004.12.015

Irie, M. S., Rabelo, G. D., Spin-Neto, R., Dechichi, P., Borges, J. S., & Soares, P. B. F. (2018). Use of micro-computed tomography for bone evaluation in dentistry. *Brazilian Dental Journal*, *29*(3), 227-238. DOI: https://doi.org/10.1590/0103-6440201801979

Jensen, T., Schou, S., Stavropoulos, A., Terheyden, H., & Holmstrup, P. (2012). Maxillary sinus floor augmentation with Bio-Oss or Bio-Oss mixed with autogenous bone as graft in animals: A systematic review. *International Journal of Oral and Maxillofacial Surgery*, *41*, 114-120. DOI: https://doi.org/10.1016/j.ijom.2011.08.010

Jones, A. C., Milthorpe, B., Averdunk, H., Limaye, A., Senden, T. J., Sakellariou, A., ... Hutmacher, D. W. (2004). Analysis of 3D bone ingrowth into polymer scaffolds via micro-computed tomography imaging. *Biomaterials*, *25*(20), 4947-4954. DOI: https://doi.org/10.1016/j.biomaterials.2004.01.047

Kamal, M., Andersson, L., Tolba, R., Al-Asfour, A., Bartella, A. K., Gremse, F., ... Lethaus, B. (2017). Bone regeneration using composite non-demineralized xenogenic dentin with beta-tricalcium phosphate in experimental alveolar cleft repair in a rabbit model. *Journal of Translational Medicine*, *15*, 263. DOI: https://doi.org/10.1186/s12967-017-1369-3

Kochi, G., Sato, S., Fukuyama, T., Morita, C., Honda, K., Arai, Y., & Ito, K. (2009). Analysis on the guided bone augmentation in the rat calvarium using a microfocus computerized tomography analysis. *Oral Surgery, Oral Medicine, Oral Pathology, Oral Radiology and Endodontology*, *107*(6), e42-e48. DOI: https://doi.org/10.1016/j.tripleo.2009.02.010

Kuchler, U., Pfingstner, G., Busenlechner, D., Dobsak, T., Reich, K., Heimel, P., & Gruber, R. (2013). Osteocyte lacunar density and area in newly formed bone of the augmented sinus. *Clinical Oral Implants Research*, *24*(3), 285-289. DOI: https://doi.org/10.1111/j.1600-0501.2012.02533.x

Lappalainen, O.-P., Karhula, S. S., Haapea, M., Kauppinen, S., Finnilä, M., Saarakkala, S., ... Sándor, G. K. (2016). Micro-CT Analysis of Bone Healing in Rabbit Calvarial Critical-Sized Defects with Solid Bioactive Glass, Tricalcium Phosphate Granules or Autogenous Bone. *Journal of Oral and Maxillofacial Research*, *7*(2). DOI: https://doi.org/10.5037/jomr.2016.7204

Lee, D. W., Koo, K. T., Seol, Y. J., Lee, Y. M., Ku, Y., Rhyu, I. C., ... Kim, T. Il. (2010). Bone regeneration effects of human allogenous bone substitutes: A preliminary study. *Journal of Periodontal and Implant Science*, *40*(3), 132-138. DOI: https://doi.org/10.5051/jpis.2010.40.3.132

Lu, M., & Rabie, A. B. M. (2004). Quantitative assessment of early healing of intramembranous and endochondral autogenous bone grafts using micro-computed tomography and Q-win image analyzer. *International Journal of Oral and Maxillofacial Surgery*, *33*(4), 369-376. DOI: https://doi.org/10.1016/j.ijom.2003.09.009

O'Hara, R. M., Orr, J. F., Buchanan, F. J., Wilcox, R. K., Barton, D. C., & Dunne, N. J. (2012). Development of a bovine collagen-Apatitic calcium phosphate cement for potential fracture treatment through vertebroplasty. *Acta Biomaterialia*, *8*(11), 4043-4052. DOI: https://doi.org/10.1016/j.actbio.2012.07.003

Ogawa, C. A., & Plepis, A. M. G. (2002). Liberação In Vitro de Cloridrato de Ciprofloxacina em Compósitos Hidroxiapatita: Colágeno. *Polímeros*, *12*(2), 115-122. DOI: https://doi.org/10.1590/s0104-14282002000200011

Olăreț, E., Stancu, I. C., Iovu, H., & Serafim, A. (2021). Computed tomography as a characterization tool for engineered scaffolds with biomedical applications. *Materials*, *14*(22), 6763. DOI: https://doi.org/10.3390/ma14226763

Pallesen, L., Schou, S., Aaboe, M., Hjørting-Hansen, E., Nattestad, A., & Melsen, F. (2002). Influence of particle size of autogenous bone grafts on the early stages of bone regeneration: a histologic and stereologic study in rabbit calvarium. *The International Journal of Oral & Maxillofacial Implants*, *17*(4), 498-506. Retrieved from http://www.ncbi.nlm.nih.gov/pubmed/12182292

Pelissier, P., Villars, F., Mathoulin-Pelissier, S., Bareille, R., Lafage-Proust, M. H., & Vilamitjana-Amedee, J. (2003). Influences of vascularization and osteogenic cells on heterotopic bone formation within a madreporic ceramic in rats. *Plastic and Reconstructive Surgery*, *111*(6), 1932-1941. DOI: https://doi.org/10.1097/01.PRS.0000055044.14093.EA

Pilliar, R. M., Filiaggi, M. J., Wells, J. D., Grynpas, M. D., & Kandel, R. A. (2001). Porous calcium polyphosphate scaffolds for bone substitute applications - In vitro characterization. *Biomaterials*, *22*(9), 963-972. DOI: https://doi.org/10.1016/S0142-9612(00)00261-1

Pripatnanont, P., Nuntanaranont, T., Vongvatcharanon, S., & Limlertmongkol, S. (2007). Osteoconductive Effects of 3 Heat-Treated Hydroxyapatites in Rabbit Calvarial Defects. *Journal of Oral and Maxillofacial Surgery*, *65*(12), 2418-2424. DOI: https://doi.org/10.1016/j.joms.2007.06.619

Redenski, I., Guo, S., MacHour, M., Szklanny, A., Landau, S., Egozi, D., ... Levenberg, S. (2022). Microcomputed Tomography-Based Analysis of Neovascularization within Bioengineered Vascularized Tissues. *ACS Biomaterials Science and Engineering*, *8*, 232-241. DOI: https://doi.org/10.1021/acsbiomaterials.1c01401

Ribas, R. G., Schatkoski, V. M., Montanheiro, T. L. do A., de Menezes, B. R. C., Stegemann, C., Leite, D. M. G., & Thim, G. P. (2019). Current advances in bone tissue engineering concerning ceramic and bioglass scaffolds: A review. *Ceramics International*, *45*(17), 21051-21061. DOI: https://doi.org/10.1016/j.ceramint.2019.07.096

Ruehe, B., Niehues, S., Heberer, S., & Nelson, K. (2009). Miniature pigs as an animal model for implant research: bone regeneration in critical-size defects. *Oral Surgery, Oral Medicine, Oral Pathology, Oral Radiology and Endodontology*, *108*(5), 699-706. DOI: https://doi.org/10.1016/j.tripleo.2009.06.037

Schmitz, J. P., Schwartza, Z., Hollinger, J. O., & Boyan, B. D. (1990). Characterization of rat calvarial nonunion defects. *Cells Tissues Organs*, *138*(3), 185-192. DOI: https://doi.org/10.1159/000146937

Sohier, J., Daculsi, G., Sourice, S., De Groot, K., & Layrolle, P. (2010). Porous beta tricalcium phosphate scaffolds used as a BMP-2 delivery system for bone tissue engineering. *Journal of Biomedical Materials Research - Part A*, *92*(3), 1105-1114. DOI: https://doi.org/10.1002/jbm.a.32467

Terheyden, H., Jepsen, S., Möller, B., Tucker, M. M., & Rueger, D. C. (1999). Sinus floor augmentation with simultaneous placement of dental implants using: A combination of deproteinized bone xenografts and recombinant human osteogenic protein-1: A histometric study in miniature pigs. *Clinical Oral Implants Research*, *10*(6), 510-521. DOI: https://doi.org/10.1034/j.1600-0501.1999.100609.x

Vásárhelyi, L., Kónya, Z., Kukovecz, & Vajtai, R. (2020). Microcomputed tomography–based characterization of advanced materials: a review. *Materials Today Advances*, *8*, 100084. DOI: https://doi.org/10.1016/j.mtadv.2020.100084

Verna, C., Bosch, C., Dalstra, M., Wikesjö, U. M. E., & Trombelli, L. (2002). Healing patterns in calvarial bone defects following guided bone regeneration in rats: A micro-CT scan analysis. *Journal of Clinical Periodontology*, *29*(9), 865-870. DOI: https://doi.org/10.1034/j.1600-051X.2002.290912.x

Wang, C., Duan, Y., Markovic, B., Barbara, J., Rolfe Howlett, C., Zhang, X., & Zreiqat, H. (2004). Proliferation and bone-related gene expression of osteoblasts grown on hydroxyapatite ceramics sintered at different temperature. *Biomaterials*, *25*(15), 2949-2956. DOI: https://doi.org/10.1016/j.biomaterials.2003.09.088

Weißenböck, M., Stein, E., Undt, G., Ewers, R., Lauer, G., & Turhani, D. (2006). Particle size of hydroxyapatite granules calcified from red algae affects the osteogenic potential of human mesenchymal stem cells in vitro. *Cells Tissues Organs*, *182*(2), 79-88. DOI: https://doi.org/10.1159/000093062

Zhi, W., Wang, X., Sun, D., Chen, T., Yuan, B., Li, X., ... Zhang, X. (2022). Optimal regenerative repair of large segmental bone defect in a goat model with osteoinductive calcium phosphate bioceramic implants. *Bioactive Materials*, *11*, 240-253. DOI: https://doi.org/10.1016/j.bioactmat.2021.09.024